coatings

MDPI

Article

A Surface Plasmon Resonance (SPR)-Based Biosensor Simulation Platform for Performance Evaluation of Different Constructional Configurations

Mariana Rodrigues Villarim [1,*], Diomadson Rodrigues Belfort [1] and Cleonilson Protasio de Souza [2]

[1] Department of Electrical Engineering, Federal University of Rio Grande do Norte, Natal 59078-970, Brazil
[2] Center for Alternative and Renewable Energy, Federal University of Paraíba, João Pessoa 58051-900, Brazil
* Correspondence: mariana.villarim.1020001@ufrn.edu.br

Abstract: Biosensors are a type of sensor that have gained prominence in recent years due to their advantages over traditional sensing methods, which are expensive and time-consuming. They are composed of two main parts: a recognizer bioelement and a transducer—both can be of different types depending on the desired application. An optical biosensor based on Surface Plasmon Resonance (SPR) achieves high sensitivity, is label-free and its multilayer construction allows an increase in the selectivity of the target analyte. As the choice of layers in SPR-based biosensors and the analysis of the obtained multilayer configuration is very difficult and expensive, in this work, we present an SPR-based biosensor simulation tool, developed through mathematical modeling, with an easy-to-use interface and several design options for calculating and analyzing the reflectance and angle of incidence of this type of device. The application, developed in Matlab, behaved as expected, offering the user the possibility to export data to Excel and becoming a useful alternative for mathematical analysis of SPR biosensors and its parameters, such as quality factor, detection accuracy and sensitivity.

Keywords: surface plasmon resonance; biosensors; simulation platform; Matlab

check for updates

Citation: Villarim, M.R.; Belfort, D.R.; de Souza, C.P. A Surface Plasmon Resonance (SPR)-Based Biosensor Simulation Platform for Performance Evaluation of Different Constructional Configurations. *Coatings* **2023**, *13*, 546. https://doi.org/10.3390/coatings13030546

Academic Editors: P. Poornesh and Feng Wang

Received: 14 January 2023
Revised: 11 February 2023
Accepted: 23 February 2023
Published: 3 March 2023

Copyright: © 2023 by the authors. Licensee MDPI, Basel, Switzerland. This article is an open access article distributed under the terms and conditions of the Creative Commons Attribution (CC BY) license (https://creativecommons.org/licenses/by/4.0/).

1. Introduction

Over the years, the medical field has been taking advantage of increasingly developed modern technologies for diagnosing diseases. The advancement of biomedicine together with sensors that are more sensitive, selective and with a shorter response time has brought new possibilities in several applications of chemical and biological sensing. In addition, health monitoring and early detection are an alternative to prevent serious and fatal illnesses such as cancer and cardiovascular disease.

Traditional methods for biochemical analysis are performed in laboratories and are expensive, time-consuming and require a specialized team [1]. Sensors of various types are being used to help assist or to replace traditional methods, forming a solution that enables real-time monitoring and can be used in remote areas [2], where it may not be possible to find a hospital nearby.

Biosensors are electronic devices that monitor biomolecular recognition events using electrochemical, optical and piezoelectric methods, among others. The advantages presented by this class of device are high specificity and real-time monitoring [3]. The main components of a biosensor can be seen in Figure 1.

Biological elements, or bioelements, are organic bodies that detect any particular analyte from the medium and must not react when coming into contact with other potentially inquisitive/interfering species, as seen in Figure 2.

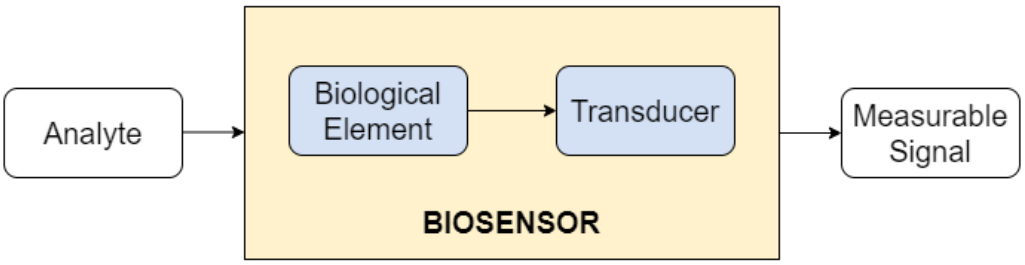

Figure 1. The main components of a biosensor.

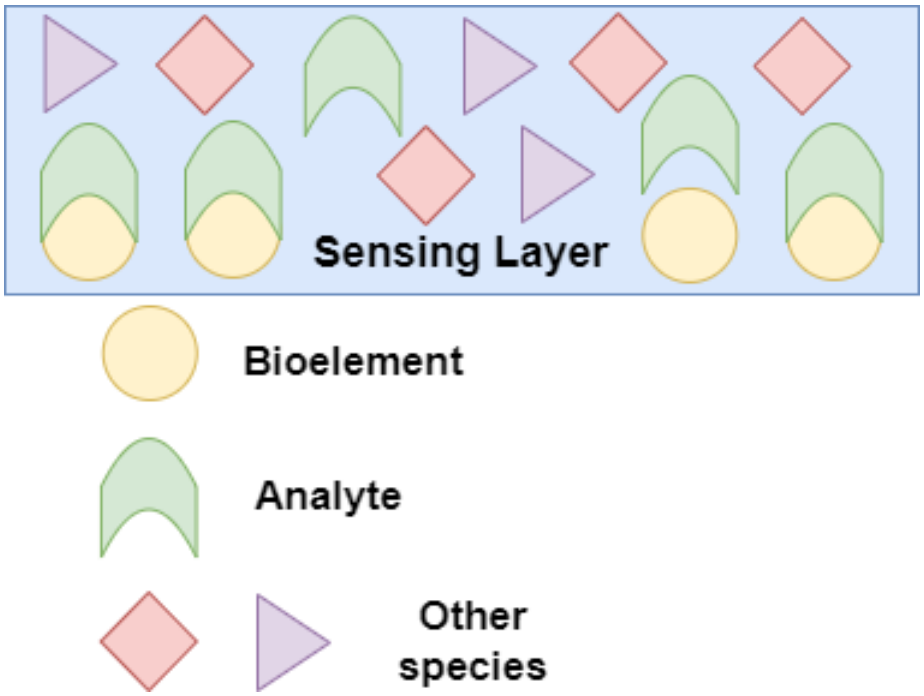

Figure 2. Operation of the sensing layer in biosensors.

Transducers are a part of the biosensor that can have varying components and have the function of transducing the energy obtained in the receptor surface into a valuable analytical signal [4], by converting interactions from an electrical signal.

Generally, after the two elements mentioned, there is a signal processing unit that contains an amplifier and a processor, which are necessary to condition and process the obtained signal [5]. A flowchart containing different types of transducers and bioelements can be seen in Figure 3.

According to the type of the chosen bioelement and the kind of transducer, biosensors can be of various types, depending on the desired application. The biological element can be an enzyme, an antibody, a nucleic acid, etc. The transducer can be electrochemical, optical, thermoelectric, piezoelectric, etc. [6].

Considering the nature of the biorecognition event, they can be classified into two groups: biocatalytic and affinity-based devices. Biocatalytic biosensors use immobilized enzymes to detect specific molecules, and affinity-based biosensors use a synthetic or biological capture agent, such as antibodies [7].

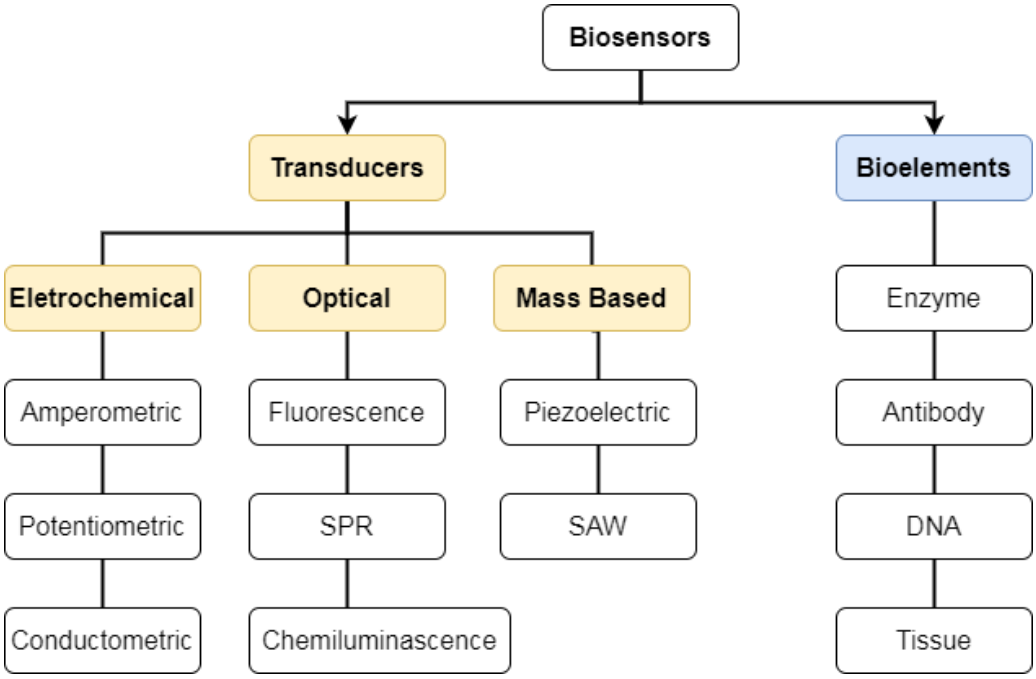

Figure 3. Different types of transducers and bioelements used in biosensors [8].

Biosensors can be classified based on constructive strategies for detection methods and can be with or without labels. Label devices are time-consuming, can alter biomolecules' binding sites and use specialized tags (colorimetric, fluorescence, chemiluminescence) to detect a specific label in the background of other materials [9]. Label-free sensors rely on material qualities such as mass, surface charge and refractive index for detection [10]. This type of sensor detects molecules directly, requiring only one recognition element [1]. Some advantages provided are high sensitivity, direct measurement of analytes, simplified sample preparation reducing consumption of organic compounds, and the opportunity for multiple sensing [9].

Label-free devices can be used in many different applications including disease diagnosis, biomedicine, food safety, environmental monitoring and security, due to their advantages of high sensitivity and resolution. They are able to diagnose infectious diseases, identify end-stage heart failure patients, perform quantitative measurement of cardiac and cancer markers, etc. The most commonly used biosensor is blood-glucose for diagnosis of *diabetes mellitus* [5].

An important type of biosensor is that based on Surface Plasmon Resonance (SPR), which is an established optical method of measuring interactions by analyzing changes in the refractive index during complex formation or dissociation of target molecules [11]. This kind of sensing has the advantage of characterizing binding reactions in real-time without labeling requirements [12] as well as its compactness, light weight and high sensitivity.

This category of sensors follows an experimental arrangement that provides a light beam able to fulfill the necessary conditions to excite a surface plasma wave in the metal–dielectric interface, and there is a necessity to evaluate the performance of the sensing system according to the displacement of minimum angle in different conditions [13], as will be described in the next section. This technique can also be combined with other types of sensing, such as electrochemical biosensors (ESPR—Electrochemical Surface Plasmon Resonance) [14].

The graph in Figure 4 presents the growth in journal publications since the year 2000, addressing the keywords "*Biosensor*", represented by blue bars, surpassing 12 thousand articles in the year 2022, and "*Surface Plasmon Resonance*", represented by red bars, surpassing 8 thousand articles on this topic in 2022. Since the year 2000, there has been an exponential growth in research on biosensors and the SPR method.

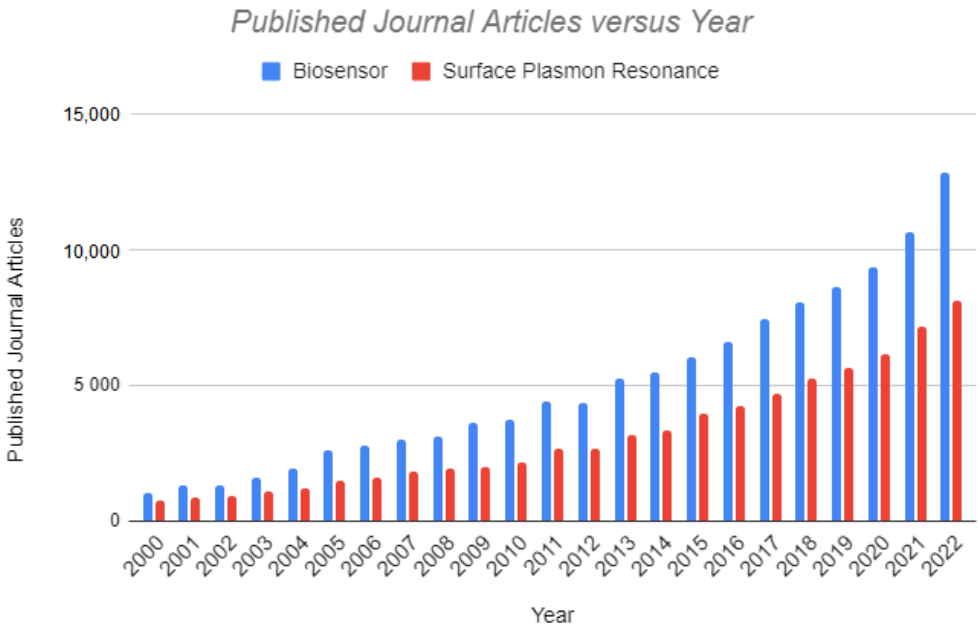

Figure 4. Growth in publications on biosensors and SPR since the year 2000. Data were obtained from the search engine *ScienceDirect*.

The vast majority of previous works, which address SPR biosensors, make use of fixed structures to analyze the sensor parameters from angle variation [15–18]. In the last decades, many methods have included materials to improve sensitivity and selectivity for biomolecules; however, there is no interactive tool providing the possibility of making this analysis simpler by adding and removing layers, for example, by varying the thickness of a certain material of the biosensor.

This paper reviews the fundamentals of SPR biosensors, their mathematical modeling and applications in detecting cardiac and cancer biomarkers. The main objective is to develop a simulation tool for SPR biosensors, which will be an interactive and easy-to-use simulation platform for the design and numerical calculation of the performance parameters of these devices, such as quality factor, sensitivity and detection accuracy. We also provide an option for exporting the output data to a spreadsheet, where it is possible to store the results of each new structure tested.

When building the sensor physically, the designer must have prior knowledge of the design parameters, such as the refractive index, incident angle and number of layers. It is highly recommended to take advantage of simulation analysis to avoid unnecessary expenses in the sensor's testing and physical implementation; therefore, our tool offers many constructive options.

The developed SPR-based biosensor simulation platform has an intuitive and easy-to-understand interface based on Matlab with options to improve the biosensor structure and obtain sensor responses, as well as the updated reflectance curve, as layers are added or removed. It is a helpful software that can be used by researchers and scientists from different areas even without previous training for data validation and simulation tests.

2. Surface Plasmon Resonance Biosensors

Surface Plasmon Resonance (SPR) is an optical phenomenon resulting from the interaction between light and electrons to detect molecular reactions, such as antigen–antibody. Such a method explores the multilayer characteristics of different types of materials according to the desired application and detection. The specification of the multilayer structure, and the definition of material and thickness, is a fundamental part in the development of SPR sensors.

Resonant oscillations of electrons occur in metallic structures when illuminated with light of a certain wavelength [19]. When a p-polarized light strikes a metal–dielectric interface, a charge density oscillation is excited, named Surface Plasmon Wave (SPW), as shown in Figure 5. This traveling surface wave is generated along the interface under resonant conditions—that is, when the momentum of the photon is equal to the momentum of the surface plasmon. A sharp dip in reflectance (SPR angle—θ_{SPR}) is observed in a resonated excitement.

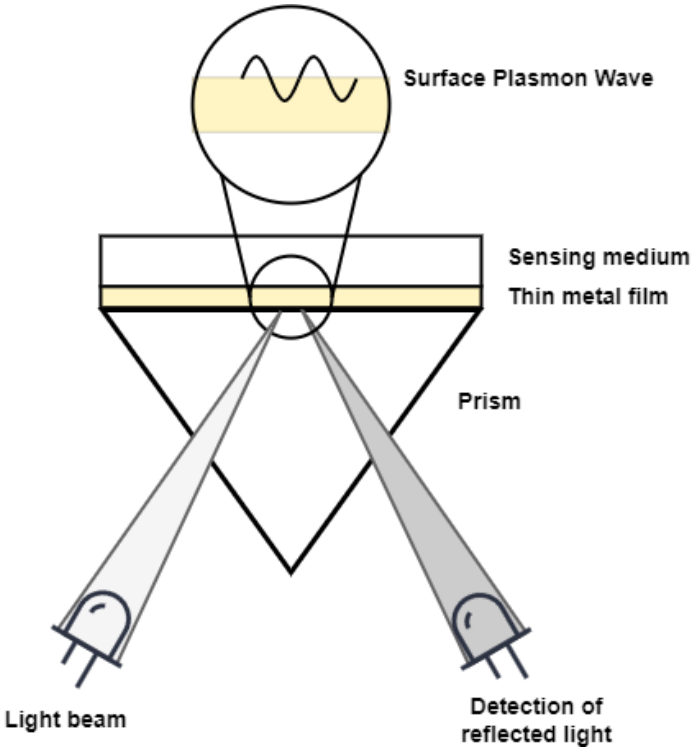

Figure 5. Light beam striking a metal–dielectric interface and generating SPW.

SPR utilizes a "chip-in-a-lab" instead of a "lab-on-a-chip" configuration due to its required use of a laser on an external prism. SPRs need precise control over the incident angle of the light to excite the plasmon on the dielectric–metal surface [20].

To satisfy Maxwell's equations that define electric and magnetic phenomena from partial differential equations, the dispersion relation for a wave propagating on the surface is given by Equation (1).

$$k_x = \frac{\omega}{c}\sqrt{\frac{\varepsilon_M \varepsilon_D}{\varepsilon_M + \varepsilon_D}} \quad (1)$$

where ω is the angular frequency, c is the speed of light in vacuum, ε_M is the dielectric function of the dielectric and ε_D is the dielectric function of the metal. The constant (β) is extremely sensitive to changes in the refractive index; it will increase at the metal surface when the biorecognition element interacts with the analyte, making its measurement by optical means possible [21].

Noble materials, such as gold and silver, are usually used as the thin metal film to activate SPWs because they exhibit free electrons. The disadvantage of a plasmonic sensor is that, because of the metallic parts, it may be plagued by strong ohmic losses, increasing its temperature and altering the analyte [22]. To overcome this drawback, some materials may be added to the structure of this type of sensor. Graphene is an absorbing material used to improve sensor performance—for example, sensitivity—as a biomolecular recognition element [23]. A graphene layer can also be used as a protective layer to prevent undesired oxidation [24].

There are two different systems developed to excite surface plasmons: the Otto configuration and the Kretschmann configuration, both displayed in Figure 6, where the latter is used in most of the commercial instruments [25]. In the Kretschmann configuration, polarized light passes through a prism to the interface, where the metal layer is in direct contact with it [25]. In Otto configuration, there is an air gap separating the prism base and the metallic layer. In both configurations, the angle of incidence varies and the angular interrogation is made, as the plasmon appears as a sharp decrease in the reflected intensity [26].

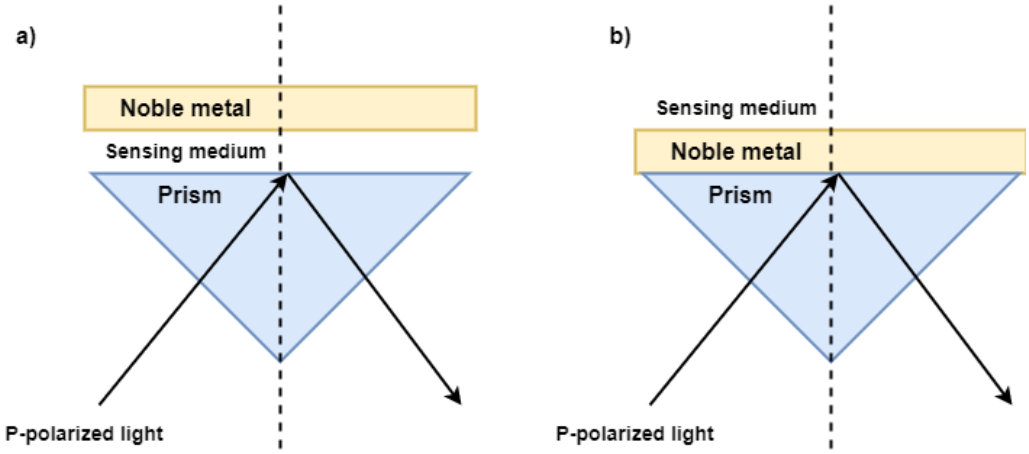

Figure 6. (**a**) Otto and (**b**) Kretschmann configurations.

When the refractive index (RI) above the metal changes by adsorption or interaction of molecules, it is possible to monitor the change in the angle of incidence so that the surface plasmon excitation occurs. The difference between the initial and final resonance angle can be seen in Figure 7 and gives an indication of the extent and rate of adsorption [27], which are used to monitor adsorption kinetics.

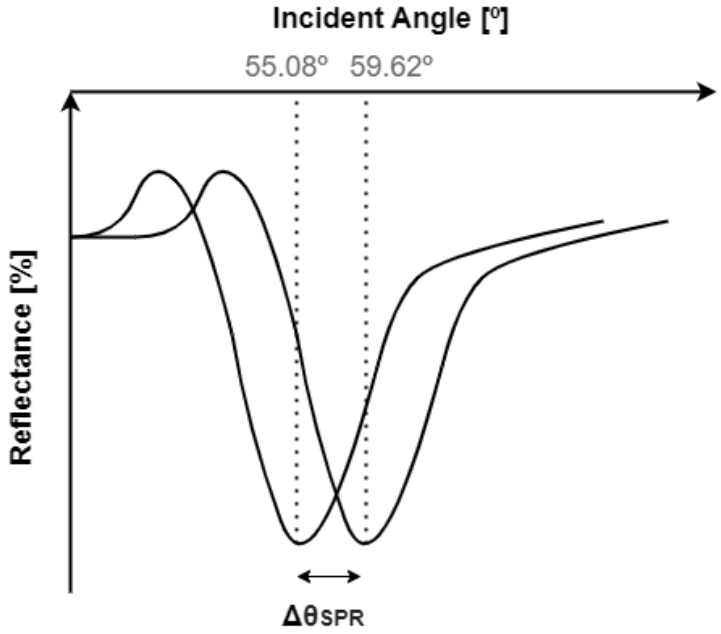

Figure 7. Change in angle value as a function of reflectance intensity.

In Figure 7, $\Delta\theta_{SPR}$ represents the change in minimum angle of reflectance. In this example, a simple structure of prism, silver and 0.06 variation of the refractive index of the

sensing medium resulted in a variation of 4.54°. The change in RI in the sensing medium after biomolecular interactions can be calculated by Equation (2).

$$n_s^a = n_s + c_a \cdot \frac{dn}{dc} \quad (2)$$

where n_s^a and n_s are the RI of sensing medium after and before adsorption, respectively; c_a is the concentration of adsorbed molecules; and $\frac{dn}{dc}$ represents the increment in RI due to the adsorbate, generally 0.182 cm³/gm when using a standard buffer solution [17].

SPR sensors based on angle modulation determine the angle of incidence—that is, the component of light's wave vector parallel to the metal surface and matching that of SPW—by measuring the coupling strength at a fixed wavelength (for example, 633 nm) and multiple incident angles of the light wave [28].

2.1. Mathematical Modeling of Surface Plasmon Resonance Biosensors

Numerical investigation and sensing performance analysis of the proposed model for the multilayer sensor is based on the Transfer Matrix Method (TMM) for the determination of reflectivity of the reflected light [29]. The matrix method does not consider approximations; so, an N-layer matrix system was used to calculate the light reflection of the prism. In Figure 8, it is possible to see a multilayer system where a light beam hits the surface of the first layer (Layer 1), part of it is reflected and part is refracted in the final layer (Layer N).

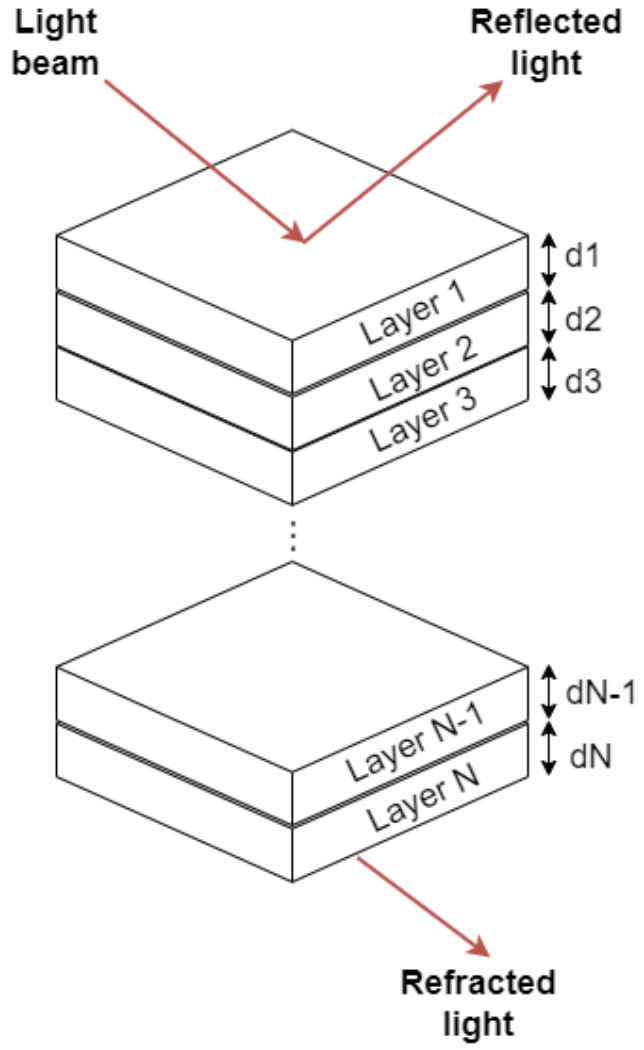

Figure 8. Multilayer SPR biosensor.

The performance of a sensor based on the SPR method can be evaluated according to parameters such as sensitivity, quality factor and detection accuracy. Changing the RI of the sample analyte causes a shift in reflectance and SPR angle [18]. The sensitivity is modified according to the angle variation of incident light and refractive index of the medium, where R_p represents reflection intensity for polarized light and can be calculated by Equation (3) using Fresnel's model analysis.

$$R_p = |r_p|^2 \tag{3}$$

The relationship of the reflection coefficient for transverse magnetically p-polarized incident light is given by Equation (4).

$$r_p = \frac{(F_{11} + F_{12}n_N)n_1 - (F_{21} + F_{22}n_N)}{(F_{11} + F_{12}n_N)n_1 + (F_{21} + F_{22}n_N)} \tag{4}$$

where n_1 and n_N are transverse refractive indices obtained from Equation (5) for the first layer and the Nth layer. The first layer represents the prism, and the Nth layer represents the sensing medium where the target molecules are located [30].

The arbitrary refractive index n_k of the corresponding kth layer can be explained by Equation (5) [31].

$$n_k = \left[\frac{\mu_k}{\varepsilon_k}\right]^{1/2} cos\theta_k = \sqrt{\frac{\varepsilon_k - (n_p sin\theta_1)^2}{\varepsilon_k^2}} \tag{5}$$

F is defined in Equation (6) as the characteristic matrix of the combined layers, θ_k is the incident angle and β_k is the arbitrary phase constant of the kth layer, as expressed in Equation (7).

$$F_{ij} = \left[\prod_{k=2}^{layers-1} \begin{pmatrix} cos\beta_k & -\frac{isin\beta_k}{n_k} \\ -in_k sin\beta_k & cos\beta_k \end{pmatrix}\right]_{ij} = \begin{bmatrix} F_{11} & F_{12} \\ F_{21} & F_{22} \end{bmatrix} \tag{6}$$

$$\beta_k = \frac{2\pi}{\lambda} d_k \sqrt{\varepsilon_k - (n_1 sin\theta_{in})^2} \tag{7}$$

where d_k is the thickness of the kth layer, n_1 is the refractive index of prism, θ_{in} is the initial incident angle and ε_k is the permittivity of kth layer. As the next topics, we will address the application of SPR biosensors in the detection of cancer and cardiac biomarkers.

2.2. SPR Biosensors Used for Cancer Biomarkers Detection

Hossain et al. [31] provided a hybrid design and numerical analysis of the graphene-coated fiber-optic SPR biosensor based on the attenuated total reflection (ATR) method for breast cancer gene-1 early onset (BRCA1) and breast cancer gene-2 early onset (BRCA2) genetic breast cancer detection by means of DNA hybridization. The graphene increased sensitivity and electric field intensity, showing that it can be more effective compared with traditional SPR biosensors. Numerical detection of cancer tumor cells was developed using two specific mutations named 916delTT and 6174delT. The study showed that the variation in SPR angle and surface plasmon frequency is considerable for complementary DNA strands and can differentiate perfectly matched and mismatched DNA interactions between the probe DNA and target DNA, which is essential for the detection of genetic biomarkers for early breast cancer, becoming a powerful and highly efficient biosensor for distinguishing cancerous cells and non-cancerous cells.

A serious problem in recent years is the frequent consumption of formalin with food, which causes severe health issues, leading to critical diseases such as chronic cancer. The detection of formalin in food is an urgent concern. Ref. [18] analyzed analytically a highly improved SPR-based sensor using graphene–MoS_2 for these applications, using attenuated total reflection (ATR) and evaluating characteristics curves of the proposed multilayer system. The results obtained through Matlab simulations showed that the sensitivity improved by 6°/RIU from the traditional sensor to the one with graphene–MoS_2 layers.

Using the same configuration proposed in the previous paper but replacing silver (Ag) with gold (Au), [17] simulated the SPR biosensor to analyze the increase in sensitivity for the detection of formalin, categorized as a Group I Carcinogen to human beings by the International Agency for Research on Cancer (IRAC). The sensitivity was observed, varying the refractive index from 1.34 to 1.41 for seven different structures of TiO_2, SiO_2, MoS_2 and graphene. It increased by 8 to 10% from the conventional structure configuration to the proposed system (conventional with graphene–MoS_2–TiO_2–SiO_2).

A review of 71 articles on SPR biosensors published in the last decade was made, focusing on cancer-specific marker testing applications and the detection of new markers, considering the validation of the developed biosensor [32]. In this study, it was concluded that sensors using the SPR method can strongly contribute to the detection of these types of biomarkers, and it was also observed that biosensors can be used to detect the stage of the disease and the evolution of cancer therapy.

2.3. SPR Biosensors Used for Cardiac Biomarkers Detection

Cardiovascular diseases (CVDs) are the leading cause of deaths, responsible for over 17.9 million each year according to the World Health Organization (WHO). Because of the high mortality and morbidity, rapid and reliable diagnosis is vital in clinical analysis [33]. Laboratory tests, such as ECGs, are expensive and time-consuming; so, there is a growing demand to find an alternative to them. A biosensor able to monitor these biomarkers provides a portable, low-cost and real-time diagnosis of cardiovascular diseases risks. According to the WHO criteria, the diagnosis of CVD must meet at least two of three conditions [34]:

- Characteristic chest pain;
- Diagnostic electrocardiogram (ECG) of typical ischemic changes;
- Elevation or decrease of the biochemical markers in blood samples.

Some proteins are released in high amounts into the bloodstream when a cardiac injury occurs and can be used as biomarkers for early diagnosis. Myoglobin is the first marker released after damage to myocardial muscle cells occurs; however, it is not very specific. Cardiac troponin I (cTnI), C-reactive protein (CRP) and B-type natriuretic peptide (BNP) are specific markers for coronary events that are released hours after myoglobin. Troponin T (TnT) is immediately released into blood circulation during a heart infarction [35].

Aiming at the early diagnosis of cardiac injury detecting troponin T (TnT), [36] combined a stable and inexpensive molecularly imprinted polymer (MIP) based on polydopamine with Surface Plasmon Resonance for preliminary experimental analysis. It achieved a linear response to the biomarker concentration with good sensitivity; however, the concentrations observed in this paper are in higher levels than those in the human bloodstream, making necessary a further work dedicated to the amplification of the detection limit.

A study developed by [33] targeted the determination of cardiac troponin I with the use of an SPR biosensor, considering the sensing ability with different concentrations of solutions. The sensor underwent experimental tests investigating selectivity for various antigens from an aqueous solution and patient serum samples. SPR sensors presented high selectivity for the cTnI biomarker and were successfully used for real-time detection, reducing costs and assay time (equilibration–adsorption–regeneration cycles) to 13.3 min.

Surface Plasmon Resonance was also used as a bioaffinity element for the detection of a novel and important cardiac biomarker: galectin-3 (Gal3). The pioneer platform was built with a gold surface, four layers of poly-(dallyldimethylammonium chloride) and graphene. Graphene has the advantage of amplifying SPR response, enhancing the analytical signal and its specificity in detection. The developed platform proved to be a competitive alternative for highly sensitive and selective label-free biosensing of Gal3 in human samples [37].

3. Development of a Simulation Tool for Analysis of SPR Biosensors

The proposed SPR biosensor is shown in Figure 9. For the sensing layer, i.e., the medium, a PBS (Phosphate-Buffered Saline) solution is chosen and the gray layers (TiO_2, SiO_2, MoS_2, graphene) are optional, being added to increase sensitivity and selectivity in the detection of the target analyte.

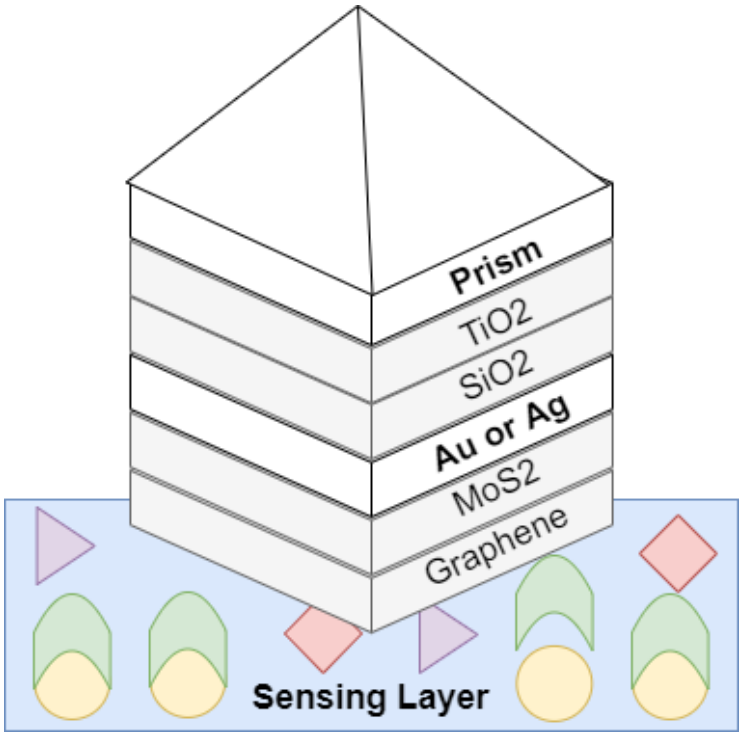

Figure 9. Graphical illustration of components of the SPR biosensor using Kretschmann configuration.

In a first analysis, considering only three layers (buffer, metal and prism), we performed a simulation to verify the variation in the minimum incidence angle (θ_{SPR}) according to refractive index at a fixed wavelength (633 nm), without considering adsorption, as shown in Figure 10.

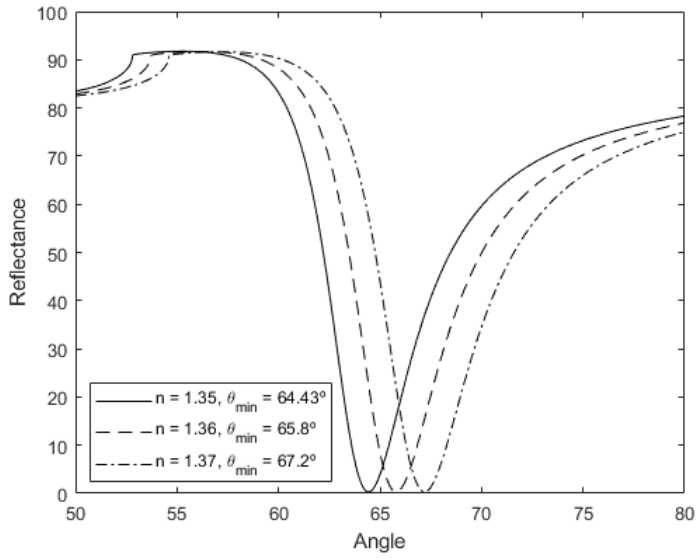

Figure 10. Variation in the minimum angle according to the change in refractive index.

This sensitivity to changes in RI is the principle of SPR biosensors. An increase in refractive index at the metal surface represents binding between biomolecular recognition elements and the target analyte, and is related to a displacement in the minimum angle of incidence. This variation from an initial minimum angle to a final angle will be used to calculate sensor parameters.

The simulation platform was developed in Matlab, utilizing the interactive development environment for application design called App Designer; then, it was exported to a script as an *.m* file. In App Designer, it is possible to organize the layout and program its behavior. The interface of the app is shown in Figure 11.

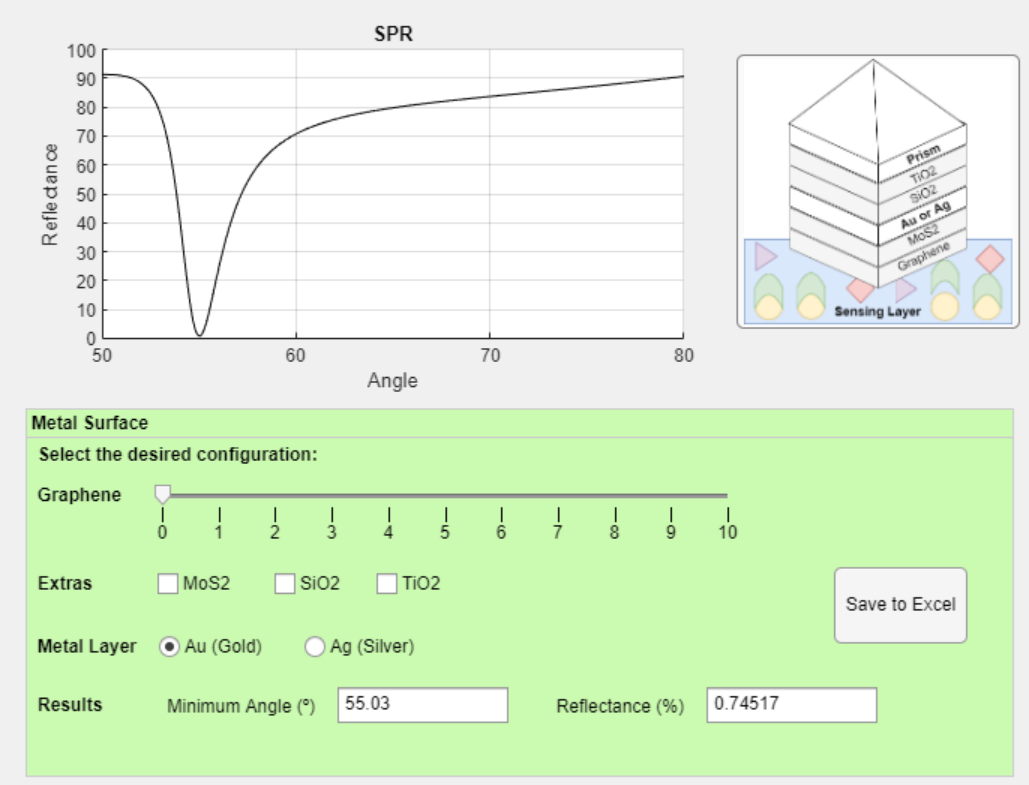

Figure 11. Initial interface of the biosensor simulator software using the SPR technique.

The user can choose the metal layer, which can be gold or silver. It also allows the user to choose whether to insert layers to improve selectivity and sensitivity, such as TiO_2 (titanium dioxide), SiO_2 (silicon dioxide), MoS_2 (molybdenum disulfide) and graphene, one of the crystalline forms of carbon. The slider bar is used to define how many graphene layers will be used, each measuring 34 nm.

We tested the proposed platform in different constructional setups to observe its operation and how the sensor responds to changes according to these variations. The user is able to visualize the minimum angle and reflectance, and also export the results to a sheet in Microsoft Excel, as shown in Figure 12.

Complex refractive index and width information for each material available are defined in Table 1 and are taken at an operating wavelength equal to 633 nm.

In Table 1, the graphene thickness is multiplied by a variable L. This variable is an integer that ranges from 0, when there are no layers of graphene, to 10. For example, by using five layers of graphene, silver as the metal layer and all the extras available to improve the detection performance of the sensor, the minimum angle and reflectance increased, as seen in Figure 13.

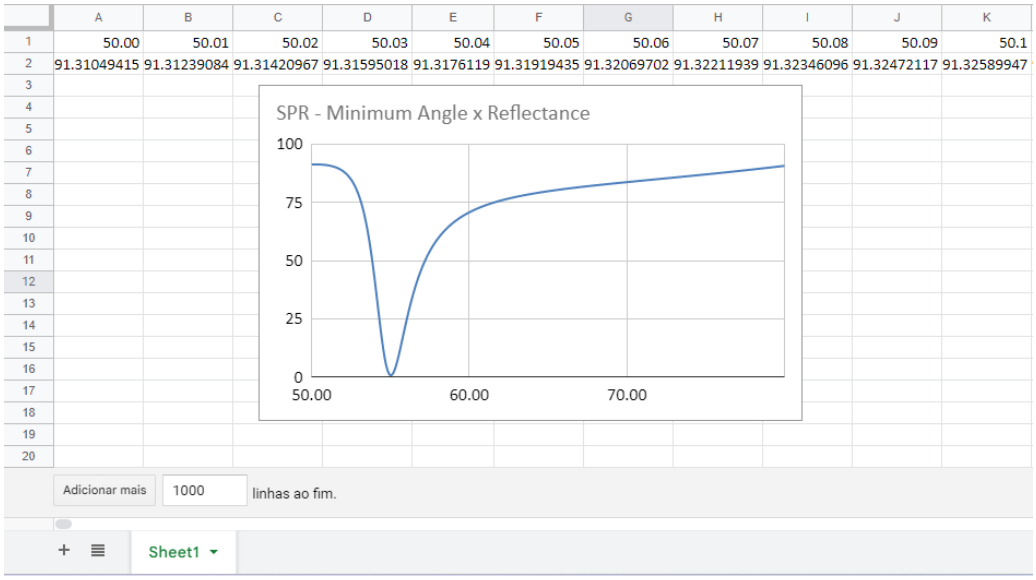

Figure 12. Data exported to Excel.

Table 1. Refractive index and width information for materials available in simulation.

Material	Complex Refractive Index	Thickness (nm)
Prism	1.7786	
TiO_2	2.5837	37 nm
SiO_2	1.4570	20 nm
Au	0.1838 + i3.4313	50 nm
Ag	0.1726 + i3.421	50 nm
MoS_2	5.9 + i0.8	0.65 nm
Graphene	3.0 + i1.1487	L*0.34 nm

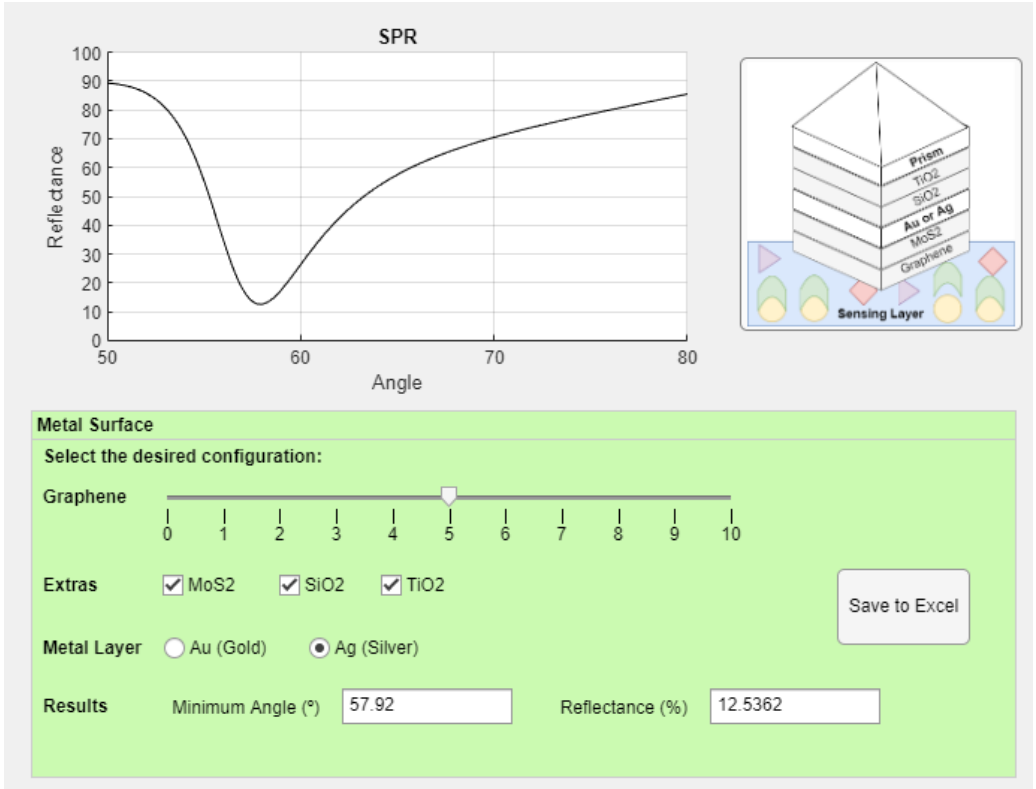

Figure 13. Simulator interface using available tools to modify the structure.

Another example is shown in Figure 14, where we have a structure with a thin metallic layer of silver, MoS_2 and only one layer of graphene. On the right side is the simulation software interface, and on the left we have the data exported to Excel, available for storage and data processing. In this case, θ_{SPR} equals 55.03º and the reflectance is 0.745%.

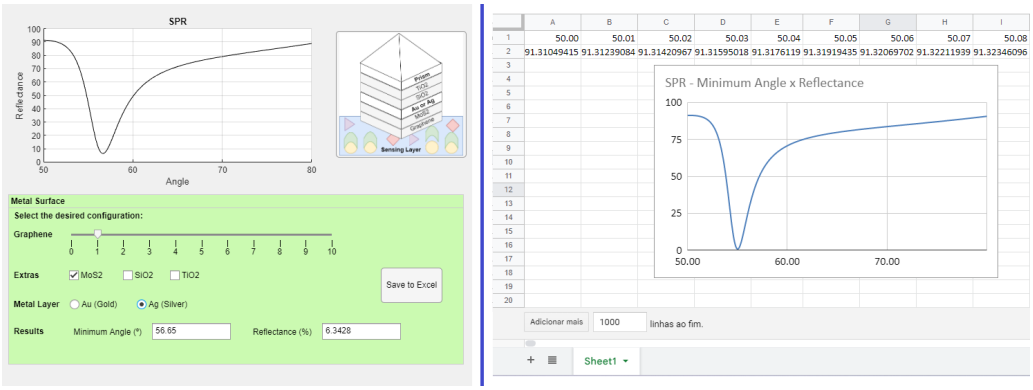

Figure 14. Interface using available tools to modify the structure: silver, one layer of graphene and MoS_2.

Table 2 lists the values of the minimum angle of incidence (θ_{SPR}, in degrees) for different constructional configurations and values of refractive index, varying the thin layer of metal between gold (Au) and silver (Ag) and with one graphene layer (when considered).

The angle and reflectance values of gold and silver are very close, as they vary only to one decimal place; what will make the designer choose between one or the other are the characteristics of the material. It is important to note that gold oxidizes less than silver in different environments but it is more expensive.

Table 2. Minimum angle of incidence for different configuration structures and refractive indexes.

Structure Configuration	Angle of Incidence (Deg)						
	***n* = 1.34**	***n* = 1.35**	***n* = 1.36**	***n* = 1.37**	***n* = 1.38**	***n* = 1.39**	***n* = 1.40**
Conventional (Ag)	55.08	55.79	56.53	57.27	58.04	58.82	59.62
Conventional (Au)	55.05	55.76	56.49	57.23	58.00	58.77	59.57
Conventional + graphene (Ag)	55.30	56.03	56.77	57.52	58.29	59.09	59.90
Conventional + graphene (Au)	55.27	55.99	56.73	57.48	58.25	59.04	59.85
Conventional + graphene + MoS_2 (Ag)	56.66	57.44	58.23	59.05	59.89	60.75	61.63
Conventional + graphene + MoS_2 (Au)	56.62	57.39	58.19	59.00	59.83	60.69	61.57
Conventional + graphene + MoS_2 + TiO_2 (Ag)	56.67	57.46	58.28	59.12	59.98	60.86	61.78
Conventional + graphene + MoS_2 + TiO_2 (Au)	56.61	57.41	58.23	59.06	59.92	60.80	61.71
Conventional + graphene + MoS_2 + TiO_2 + SiO_2 (Ag)	56.70	57.50	58.32	59.16	60.02	60.91	61.83
Conventional + graphene + MoS_2 + TiO_2 + SiO_2 (Au)	56.64	57.45	58.27	59.10	59.96	60.85	61.77

The performance of the SPR sensor can be characterized by three main parameters [38]:

- Sensitivity;
- Quality factor;
- Detection accuracy.

Sensitivity (S) is an important performance characteristic parameter and can be calculated using Equation (8) by the ratio of the shift in sensor output (angle of incidence) to

the change in refractive index in the sensing region (analyte concentration). The unit is expressed as deg/RIU. This parameter should be as high as possible in a good sensor.

$$S = \frac{\Delta\theta_{spr}}{\Delta n_a} \tag{8}$$

Detection accuracy (D.A., also known as signal-to-noise ratio) can be calculated using Equation (9) by the ratio of the shift in sensor output to the full width at half maximum (FWHM) of the reflectance curve and is a dimensionless parameter.

$$D.A. = \frac{\Delta\theta_{SPR}}{\Delta\theta_{0.5}} \tag{9}$$

where $\Delta\theta_{0.5}$ is the spectral width of the curve corresponding to 50% reflectivity.

The quality factor (Q.F.) of the proposed sensor can be calculated by Equation (10) and is defined as the ratio of sensitivity to $\Delta\theta_{0.5}$.

$$Q.F. = \frac{S}{\Delta\theta_{0.5}} \tag{10}$$

Table 3 lists the sensitivity values for the different structure configurations for both silver and gold, considering refractive indexes varying from 1.34 to 1.40. To calculate sensitivity, it was necessary to measure the minimum angle of incidence in different refractive indexes; calculate the differences between them; and finally, divide by the difference between the RIs (0.06).

Table 3. Sensitivity parameter values calculated for different structure configurations.

Structure Configuration	θ_{res} (Deg)		$\Delta\theta_{res}$ (Deg)	S
	n = 1.34	*n = 1.40*	Δ_{n_s} *= 0.06*	[°/RIU]
Conventional (Ag)	55.08	59.62	4.54	75.67
Conventional (Au)	55.05	59.57	4.52	73.33
Conventional + graphene (Ag)	55.30	59.90	4.60	76.67
Conventional + graphene (Au)	55.27	59.85	4.58	76.33
Conventional + graphene + MoS_2 (Ag)	56.65	61.63	4.98	83
Conventional + graphene + MoS_2 (Au)	56.62	61.57	4.95	82.5
Conventional + graphene + MoS_2 + TiO_2 (Ag)	56.67	61.78	5.11	85.17
Conventional + graphene + MoS_2 + TiO_2 (Au)	56.61	61.71	5.10	85
Conventional + graphene + MoS_2 + TiO_2 + SiO_2 (proposed) (Ag)	56.70	61.83	5.13	85.50
Conventional + graphene + MoS_2 + TiO_2 + SiO_2 (proposed) (Au)	56.64	61.77	5.13	85.50

The percentage increase in sensitivity for the conventional structure configuration over the proposed structure configuration containing all layers is 12.99% for silver and 16.59% for gold. Table 4 lists values for detection accuracy and quality factor for a refractive index equal to 1.34.

Table 4. Detection accuracy and quality factor values for different structure configurations.

Structure Configuration	@ n = 1.34		FWHM (Deg)	D.A.	Q.F.
	θ_{low} (Deg)	θ_{high} (Deg)			
Conventional (Ag)	53.82	57.46	3.64	1.25	20.79
Conventional (Au)	53.76	57.52	3.76	1.20	19.50
Conventional + graphene (Ag)	53.90	57.97	4.07	1.13	18.84
Conventional + graphene (Au)	53.84	58.05	4.21	1.09	18.13
Conventional + graphene + MoS_2 (Ag)	54.62	60.84	6.22	0.80	13.34
Conventional + graphene + MoS_2 (Au)	54.55	60.96	6.41	0.77	12.87
Conventional + graphene + MoS_2 + TiO_2 (Ag)	54.58	60.67	6.09	0.84	13.98
Conventional + graphene + MoS_2 + TiO_2 (Au)	54.51	60.76	6.25	0.82	13.60
Conventional + graphene + MoS_2 + TiO_2 + SiO_2 (proposed) (Ag)	54.50	61.49	6.99	0.74	12.23
Conventional + graphene + MoS_2 + TiO_2 + SiO_2 (proposed) (Au)	54.43	61.62	7.19	0.71	11.89

The values of sensor parameters for silver and gold are very similar; so, the choice of the designer will depend on the characteristics of each material. As listed in Table 3 and Table 4, when adding layers with different types of materials, the sensitivity increased but the detection accuracy and quality factor decreased because of the growth in full width at half maximum, generating a larger dip in the curve. Therefore, there must be a trade-off in the possibilities.

4. Conclusions

Surface Plasmon Resonance sensors are a special type of optical biosensor that can be applied in different areas, such as the medical, food and environmental industries, and has many types of applications. In the medical area, it can be used as an alternative to traditional laboratory tests that are expensive and time-consuming. We reviewed papers that proved that these devices successfully monitor cancer and cardiac biomarkers and have the advantage of being portable, low-cost and provide real-time diagnosis, reducing mortality and morbidity.

Thus, we developed an easy-to-use platform for multilayer SPR biosensors using Matlab software. This interactive simulation tool offers the user possibilities to increase sensitivity by adding layers to the sensor configuration, providing data on the minimum incidence angle and reflectance, and the ability to export data to a table in Excel to be processed. With the data provided, we were able to calculate the sensitivity, detection accuracy and quality factor for five different sensor configurations, considering both silver and gold as noble materials.

When increasing the multilayer system with different materials, we observed a growth in sensitivity of 12.99% for silver and 16.59% for gold, but D.A. and Q.F. decreased because of the increased width in the dip of the minimum incidence angle curve.

The optimization of SPR biosensors has been studied for years, modifying the structure to include certain materials that contribute to the sensitivity and selectivity in the detection of biomolecules. However, the developed interface presents an interactive alternative for simulating different SPR devices, where the user can modify the multilayer structure and observe the variations in the performance parameters.

Therefore, mathematical modeling proved to be very important in a project to predict experimental behavior via simulation, reducing expenses when testing and choosing the best structure configuration for a given application, respecting the trade-offs between its parameters.

5. Future Perspectives

Our main focus in future perspectives is the analysis of data acquisition and processing, with experimental procedures in different human samples, to verify if the resolution and sensitivity of the systems simulated are far from reality. Another investigation to be conducted will be the addition of noise sources to verify the contribution to the resolution and detection accuracy of the system.

A physical modeling for the design and analysis of the proposed model based on finite differences time domain (FDTD) will be addressed. FDTD, used for solving Maxwell's equations, produces the dispersion ratio for the surface of a metal adjacent to a medium such as air or vacuum, determining the propagation of the electromagnetic wave in all the layers that compose it. FDTD has a drawback related to unbounded domains; thus, it will be necessary to implement radiation boundary conditions, such as the Perfectly Matched Layer (PML) method.

Author Contributions: Conceptualization, M.R.V., D.R.B. and C.P.d.S.; Methodology, M.R.V.; Software, M.R.V.; Validation, M.R.V.; Writing—original draft, M.R.V.; Writing—review & editing, D.R.B. and C.P.d.S.; Visualization, D.R.B. and C.P.d.S.; Supervision, D.R.B. and C.P.d.S. All authors have read and agreed to the published version of the manuscript.

Funding: This research was funded by Coordenação de Aperfeiçoamento de Pessoal de Nível Superior-CAPES grant number 001.

Data Availability Statement: No new data were created or analyzed in this study. Data sharing is not applicable to this article.

Conflicts of Interest: The authors declare no conflict of interest. The funders had no role in the design of the study; in the collection, analyses, or interpretation of data; in the writing of the manuscript; or in the decision to publish the results.

References

1. Andryukov, B.G.; Besednova, N.N.; Romashko, R.V.; Zaporozhets, T.S.; Efimov, T.A. Label-free biosensors for laboratory-based diagnostics of infections: Current achievements and new trends. *Biosensors* **2020**, *10*, 11. [CrossRef] [PubMed]
2. Albahri, O.S.; Albahri, A.S.; Mohammed, K.; Zaidan, A.; Zaidan, B.; Hashim, M.; Salman, O.H. Systematic review of real-time remote health monitoring system in triage and priority-based sensor technology: Taxonomy, open challenges, motivation and recommendations. *J. Med. Syst.* **2018**, *42*, 80. [CrossRef] [PubMed]
3. Helmerhorst, E.; Chandler, D.J.; Nussio, M.; Mamotte, C.D. Real-time and label-free bio-sensing of molecular interactions by surface plasmon resonance: A laboratory medicine perspective. *Clin. Biochem. Rev.* **2012**, *33*, 161. [PubMed]
4. Ali, J.; Najeeb, J.; Ali, M.A.; Aslam, M.F.; Raza, A. Biosensors: Their fundamentals, designs, types and most recent impactful applications: A review. *J. Biosens. Bioelectron.* **2017**, *8*, 235. [CrossRef]
5. Mehrotra, P. Biosensors and their applications–A review. *J. Oral Biol. Craniofacial Res.* **2016**, *6*, 153–159. [CrossRef]
6. Meshram, B.; Agrawal, A.; Adil, S.; Ranvir, S.; Sande, K. Biosensor and its application in food and dairy industry: A review. *Int. J. Curr. Microbiol. Appl. Sci.* **2018**, *7*, 3305–3324. [CrossRef]
7. Victorious, A.; Saha, S.; Pandey, R.; Didar, T.F.; Soleymani, L. Affinity-based detection of biomolecules using photo-electrochemical readout. *Front. Chem.* **2019**, *7*, 617. [CrossRef]
8. Tetyana, P.; Shumbula, P.M.; Njengele-Tetyana, Z. Biosensors: Design, Development and Applications. In *Nanopores*; IntechOpen: London, UK, 2021.
9. Sang, S.; Wang, Y.; Feng, Q.; Wei, Y.; Ji, J.; Zhang, W. Progress of new label-free techniques for biosensors: A review. *Crit. Rev. Biotechnol.* **2016**, *36*, 465–481. [CrossRef]
10. Samuel, V.R.; Rao, K.J. A review on label free biosensors. *Biosens. Bioelectron. X* **2022**, *11*, 100216. [CrossRef]
11. Chau, Y.F.C. Mid-infrared sensing properties of a plasmonic metal–insulator–metal waveguide with a single stub including defects. *J. Phys. D Appl. Phys.* **2020**, *53*, 115401. [CrossRef]
12. Rich, R.L.; Myszka, D.G. Advances in surface plasmon resonance biosensor analysis. *Curr. Opin. Biotechnol.* **2000**, *11*, 54–61. [CrossRef]
13. Rodríguez-Schwendtner, E.; González-Cano, A.; Díaz-Herrera, N.; Navarrete, M.; Esteban, Ó. Signal processing in SPR fiber sensors: Some remarks and a new method. *Sens. Actuators B Chem.* **2018**, *268*, 150–156. [CrossRef]
14. Golden, J.; Yates, M.D.; Halsted, M.; Tender, L. Application of electrochemical surface plasmon resonance (ESPR) to the study of electroactive microbial biofilms. *Phys. Chem. Chem. Phys.* **2018**, *20*, 25648–25656. [CrossRef] [PubMed]
15. Zhao, X.; Huang, T.; Ping, P.S.; Wu, X.; Huang, P.; Pan, J.; Wu, Y.; Cheng, Z. Sensitivity enhancement in surface plasmon resonance biochemical sensor based on transition metal dichalcogenides/graphene heterostructure. *Sensors* **2018**, *18*, 2056. [CrossRef]
16. Xia, G.; Zhou, C.; Jin, S.; Huang, C.; Xing, J.; Liu, Z. Sensitivity enhancement of two-dimensional materials based on genetic optimization in surface plasmon resonance. *Sensors* **2019**, *19*, 1198. [CrossRef]
17. Hossain, M.B.; Rana, M.M.; Abdulrazak, L.F.; Mitra, S.; Rahman, M. Graphene-MoS_2 with TiO_2SiO_2 layers based surface plasmon resonance biosensor: Numerical development for formalin detection. *Biochem. Biophys. Rep.* **2019**, *18*, 100639. [CrossRef]
18. Moznuzzaman, M.; Islam, M.R.; Hossain, M.B.; Mehedi, I.M. Modeling of highly improved SPR sensor for formalin detection. *Results Phys.* **2020**, *16*, 102874. [CrossRef]
19. Chau, Y.F.; Yeh, H.H.; Tsai, D. Surface plasmon resonances effects on different patterns of solid-silver and silver-shell nanocylindrical pairs. *J. Electromagn. Waves Appl.* **2010**, *24*, 1005–1014. [CrossRef]
20. Pitruzzello, G.; Krauss, T.F. Photonic crystal resonances for sensing and imaging. *J. Opt.* **2018**, *20*, 073004. [CrossRef]
21. Homola, J. Present and future of surface plasmon resonance biosensors. *Anal. Bioanal. Chem.* **2003**, *377*, 528–539. [CrossRef]
22. Tognazzi, A.; Rocco, D.; Gandolfi, M.; Locatelli, A.; Carletti, L.; De Angelis, C. High quality factor silicon membrane metasurface for intensity-based refractive index sensing. *Optics* **2021**, *2*, 18. [CrossRef]
23. Verma, A.; Prakash, A.; Tripathi, R. Sensitivity enhancement of surface plasmon resonance biosensor using graphene and air gap. *Opt. Commun.* **2015**, *357*, 106–112. [CrossRef]
24. Choi, S.H.; Kim, Y.L.; Byun, K.M. Graphene-on-silver substrates for sensitive surface plasmon resonance imaging biosensors. *Opt. Express* **2011**, *19*, 458–466. [CrossRef] [PubMed]
25. Schasfoort, R.B. *Handbook of Surface Plasmon Resonance*; Royal Society of Chemistry: London, UK, 2017.
26. Estroff, A.; Smith, B.W. Tuning metamaterials for applications at DUV wavelengths. *Int. J. Opt.* **2012**, *2012*, 603083. [CrossRef]
27. Carvalho, R.M.d.; Rath, S.; Kubota, L.T. SPR: Uma nova ferramenta para biossensores. *Química Nova* **2003**, *26*, 97–104. [CrossRef]

28. Rahman, M.S.; Anower, M.; Rahman, M.K.; Hasan, M.R.; Hossain, M.B.; Haque, M.I. Modeling of a highly sensitive MoS_2-Graphene hybrid based fiber optic SPR biosensor for sensing DNA hybridization. *Optik* **2017**, *140*, 989–997. [CrossRef]
29. Maurya, J.; Prajapati, Y.; Singh, V.; Saini, J. Sensitivity enhancement of surface plasmon resonance sensor based on graphene–MoS_2 hybrid structure with TiO_2–SiO_2 composite layer. *Appl. Phys. A* **2015**, *121*, 525–533. [CrossRef]
30. Kumar, R.; Pal, S.; Verma, A.; Prajapati, Y.; Saini, J. Effect of silicon on sensitivity of SPR biosensor using hybrid nanostructure of black phosphorus and MXene. *Superlattices Microstruct.* **2020**, *145*, 106591. [CrossRef]
31. Hossain, M.B.; Islam, M.M.; Abdulrazak, L.F.; Rana, M.M.; Akib, T.B.A.; Hassan, M. Graphene-coated optical fiber SPR biosensor for BRCA1 and BRCA2 breast cancer biomarker detection: A numerical design-based analysis. *Photonic Sens.* **2020**, *10*, 67–79. [CrossRef]
32. Falkowski, P.; Lukaszewski, Z.; Gorodkiewicz, E. Potential of surface plasmon resonance biosensors in cancer detection. *J. Pharm. Biomed. Anal.* **2021**, *194*, 113802. [CrossRef]
33. Çimen, D.; Bereli, N.; Günaydın, S.; Denizli, A. Detection of cardiac troponin-I by optic biosensors with immobilized anti-cardiac troponin-I monoclonal antibody. *Talanta* **2020**, *219*, 121259. [CrossRef] [PubMed]
34. Al-Hadi, H.A.; Fox, K.A. Cardiac markers in the early diagnosis and management of patients with acute coronary syndrome. *Sultan Qaboos Univ. Med. J.* **2009**, *9*, 231. [PubMed]
35. Qureshi, A.; Gurbuz, Y.; Niazi, J.H. Biosensors for cardiac biomarkers detection: A review. *Sens. Actuators B Chem.* **2012**, *171*, 62–76. [CrossRef]
36. Palladino, P.; Minunni, M.; Scarano, S. Cardiac Troponin T capture and detection in real-time via epitope-imprinted polymer and optical biosensing. *Biosens. Bioelectron.* **2018**, *106*, 93–98. [CrossRef]
37. Primo, E.N.; Kogan, M.J.; Verdejo, H.E.; Bollo, S.; Rubianes, M.D.; Rivas, G.A. Label-free graphene oxide-based surface plasmon resonance immunosensor for the quantification of galectin-3, a novel cardiac biomarker. *ACS Appl. Mater. Interfaces* **2018**, *10*, 23501–23508. [CrossRef]
38. Basak, C.; Hosain, M.K.; Sazzad, A.A. Design and simulation of a high sensitive surface plasmon resonance biosensor for detection of biomolecules. *Sens. Imaging* **2020**, *21*, 2. [CrossRef]

Disclaimer/Publisher's Note: The statements, opinions and data contained in all publications are solely those of the individual author(s) and contributor(s) and not of MDPI and/or the editor(s). MDPI and/or the editor(s) disclaim responsibility for any injury to people or property resulting from any ideas, methods, instructions or products referred to in the content.